water-in-octane solubility data[28] place a lower limit on this barrier of 40 kJ mol$^{-1}$.

Results from the water–1-octanol system also provide insight into methods used to characterize the membrane affinity of different pharmaceutical and natural products. The 'log$P$' scale describes a solute's tendency to partition across a water–1-octanol interface, and has been used for almost 70 years as a measure of biological activity[29]. This scale evolved from empirical searches for systems that correlated with known physiological efficacy of different anaesthetics. The spectra in Fig. 3 imply that the success of the 'log$P$' scale may, in part, be due to a membrane-like structure induced in the interfacial octanol solvent by the underlying aqueous phase.

The present experiments have used a family of surfactants to determine how solvent polarity changes across weakly and strongly associating liquid–liquid interfaces. Using resonance-enhanced SHG, we measure probe excitation wavelengths as a function of probe–headgroup separation. Solvent polarity across the weakly associating, water–cyclohexane interface smoothly converges from the aqueous to the organic limit in less than 9 Å. This result supports existing models of molecularly sharp interfaces proposed by simulations and X-ray scattering results. The strongly associating, water–1-octanol interface presents a region that is considerably less polar than either bulk phase, implying that surface-induced ordering of the organic solvent creates a hydrophobic barrier between the two polar liquids. ☐

1. Viceli, J. & Benjamin, I. Adsorption at the interface between water and self-assembled monolayers: Structure and electronic spectra. *J. Phys. Chem. B* **106**, 7898–7907 (2002).
2. Chang, T. M. & Dang, L. X. Molecular dynamics simulations of CCl₄-H₂O liquid-liquid interface with polarizable potential models. *J. Chem. Phys.* **104**, 6772–6783 (1996).
3. Chipot, C., Wilson, M. A. & Pohorille, A. Interactions of anesthetics with the water-hexane interface. A molecular dynamics study. *J. Phys. Chem. B* **101**, 782–791 (1997).
4. DaRocha, S. R. & Rossky, P. J. Surfactant modified CO₂-water interface: A molecular view. *J. Phys. Chem. B* **106**, 13250–13261 (2002).
5. Senapati, S. & Berkowitz, M. L. Computer simulation study of the interface width of the liquid/liquid interface. *Phys. Rev. Lett.* **87**, 176101 (2001).
6. Lee, L. T., Langevin, D. & Farnoux, B. Neutron reflectivity at liquid interfaces. *Physica B* **198**, 83–88 (1994).
7. Penfold, J., Richardson, R. M., Zarbakhsh, A. & Webster, J. R. P. Recent advances in the study of chemical surfaces and interfaces by specular neutron reflection. *J. Chem. Soc. Faraday Trans.* **93**, 3899–3917 (1997).
8. Tikhonov, A. M., Mitrinovic, D. M., Li, M., Huang, Z. & Schlossman, M. L. An X-ray reflectivity study of the water-docosane interface. *J. Phys. Chem. B* **104**, 6336–6339 (2000).
9. Steel, W. H., Damkaci, F., Nolan, R. & Walker, R. A. Molecular rulers: New families of molecules for measuring interfacial widths. *J. Am. Chem. Soc.* **124**, 4824–4831 (2002).
10. Antoine, A., Bianchi, F., Brevet, P. F. & Girault, H. H. Studies of water/alcohol and air/alcohol interfaces by second harmonic generation. *J. Chem. Soc. Faraday Trans.* **93**, 3833–3838 (1997).
11. Corn, R. M. & Higgins, D. A. Optical second harmonic spectroscopy as a probe of surface chemistry. *Chem. Rev.* **94**, 107–125 (1994).
12. Eisenthal, K. B. Photochemistry and photophysics of liquid interfaces by second harmonic spectroscopy. *J. Phys. Chem.* **100**, 12997–13006 (1996).
13. Zhuang, X., Miranda, P. B., Kim, D. & Shen, Y. R. Mapping molecular orientation and conformation at interfaces by surface nonlinear optics. *Phys. Rev. B* **59**, 12632–12640 (1999).
14. Laurence, C., Nicolet, P. & Dalati, M. T. The empirical treatment of solvent-solute interactions: 15 years of π*. *J. Phys. Chem.* **98**, 5807–5816 (1994).
15. Shen, Y. R. Surface properties probed by second harmonic and sum frequency generation. *Nature* **337**, 519–525 (1989).
16. Wang, H., Borguet, E. & Eisenthal, K. B. Polarity of liquid interfaces by second harmonic generation spectroscopy. *J. Phys. Chem. A* **101**, 713–718 (1997).
17. Wang, H., Borguet, E. & Eisenthal, K. B. Generalized interface polarity scale based on second harmonic spectroscopy. *J. Phys. Chem. B* **102**, 4927–4932 (1998).
18. Ishizaka, S., Kim, H. B. & Kitamura, N. Time-resolved total internal reflection fluorometry study on polarity at a liquid/liquid interface. *Anal. Chem.* **73**, 2421–2428 (2001).
19. Benjamin, I. Solvent effects on electronic spectra at liquid interfaces. A continuum electrostatic model. *J. Phys. Chem. A* **102**, 9500–9506 (1998).
20. Steel, W. H. & Walker, R. A. Solvent polarity at an aqueous/alkane interface: The effect of solute identity. *J. Am. Chem. Soc.* **125**, 1132–1133 (2003).
21. Li, Z. X., Bain, C. D., Thomas, R. K., Duffy, D. C. & Penfold, J. Monolayers of hexadecyltrimethylammonium p-tosylate at the air-water interface 2. Neutron reflection. *J. Phys. Chem. B* **102**, 9473–9480 (1998).
22. Penfold, J. & Thomas, R. K. Solvent distribution in non-ionic surfactant monolayers. *Phys. Chem. Chem. Phys.* **4**, 2648–2652 (2002).
23. Tikhonov, A. M. & Schlossman, M. L. Surfactant and water ordering in triacontanol monolayers at the water-hexane interface. *J. Phys. Chem. B* **107**, 3344–3347 (2003).
24. Schweighofer, K., Essmann, U. & Berkowitz, M. Simulation of sodium dodecyl sulfate at the water-

vapor and water-carbon tetrachloride interfaces at low surface coverages. *J. Phys. Chem. B* **101**, 3793–3799 (1997).
25. Zhang, X. & Walker, R. A. Discrete partitioning of solvent permittivity at liquid-solid interfaces. *Langmuir* **17**, 4486–4489 (2001).
26. Zhang, Z., Mitrinovic, D. M., Williams, S. M., Huang, Z. & Schlossman, M. L. X-ray scattering from monolayers of F(CF₂)₁₀(CH₂)₂OH at the water-(hexane solution) and water-vapor interfaces. *J. Chem. Phys.* **110**, 7421–7432 (1999).
27. Barton, A. F. M. (ed.) *IUPAC Solubility Data Series: Alcohols with Water* (Pergamon, Oxford, 1984).
28. Tsonopoulos, C. & Wilson, G. M. High-temperature mutual solubilities of hydrocarbons and water. *Am. Inst. Chem. J.* **31**, 376–384 (1983).
29. Sangster, J. *Octanol-Water Partition Coefficients* (ed. Fogg, P. G. T.) 2–15 (Wiley and Sons, New York, 1997).

**Correspondence** and requests for materials should be addressed to R.A.W. (rw158@umail.umd.edu).

· · · · · · · · · · · · · · · · · · · · · · · · · · · · · · · · · · · · · · · · · · · · ·

# Palaeoceanographic implications of genetic variation in living North Atlantic *Neogloboquadrina pachyderma*

**D. Bauch***, **K. Darling**†, **J. Simstich***, **H.A. Bauch***‡, **H. Erlenkeuser**§ & **D. Kroon**∥

* *GEOMAR, Wischhofstrasse 1-3, 24148-Kiel, Germany*
† *School of GeoSciences and Institute of Cell, Animal & Population Biology, University of Edinburgh, West Mains Road, Edinburgh EH9 3JG, UK*
‡ *Mainz Academy of Sciences, Humanity and Literature, Geschwister-Scholl-Strasse 2, 55131-Mainz, Germany*
§ *Leibniz Laboratory, Kiel University, Max-Eyth Strasse, 24118-Kiel, Germany*
∥ *Vrije Universiteit Amsterdam, De Boelelaan 1085, N-1081 HV Amsterdam, The Netherlands*

**The shells of the planktonic foraminifer *Neogloboquadrina pachyderma* have become a classical tool for reconstructing glacial–interglacial climate conditions in the North Atlantic Ocean[1–3]. Palaeoceanographers utilize its left- and right-coiling variants, which exhibit a distinctive reciprocal temperature and water mass related shift in faunal abundance both at present and in late Quaternary sediments[1,2,4,5]. Recently discovered cryptic genetic diversity in planktonic foraminifers[6–8] now poses significant questions for these studies. Here we report genetic evidence demonstrating that the apparent 'single species' shell-based records of right-coiling *N. pachyderma* used in palaeoceanographic reconstructions contain an alternation in species as environmental factors change. This is reflected in a species-dependent incremental shift in right-coiling *N. pachyderma* shell calcite δ$^{18}$O between the Last Glacial Maximum and full Holocene conditions. Guided by the percentage dextral coiling ratio, our findings enhance the use of δ$^{18}$O records of right-coiling *N. pachyderma* for future study. They also highlight the need to genetically investigate other important morphospecies to refine their accuracy and reliability as palaeoceanographic proxies.**

Morphological distinction provides the main basis for foraminiferal counts and derived palaeoceanographic reconstructions[2,9,10], and yet the genus *Neogloboquadrina* is known to be a rather variable morphogroup[5,11–14]. Although lack of DNA in fossil foraminiferal shells precludes genetic investigation, molecular analyses of the

living *N. pachyderma* planktonic assemblages now provide the opportunity to resolve much of this confusion. The left-coiling ('sin.') form of the morphospecies *N. pachyderma* is the dominant morphotype today in the cold, high-northern latitudes[15,16] (Fig. 1a). Although right-coiling ('dex.') *N. pachyderma* is found in more temperate environments than its left-coiled counterpart (Fig. 1a), a small percentage of *N. pachyderma* (dex.) persists in sedimentary records, even in regions with extreme polar conditions such as the central Arctic Ocean[17]. It is unknown whether these *N. pachyderma* (dex.) represent sporadic hydrographic change, expatriation from their more-temperate water mass, or whether they are aberrant forms of the left-coiling variety. Recently, the $\delta^{18}O$ signature in *N. pachyderma* (dex.) has been proposed as a good recorder of glacial–interglacial sea surface temperatures[18–20]. Our molecular work now questions such continuous 'single species' use of the *N. pachyderma* (dex.) $\delta^{18}O$ record for past climate reconstruction. We have investigated this species-versus-morphology issue by comparing the genotypic identity of *N. pachyderma* (sin. and dex.) collected from the Nordic seas surface waters against a background of *N. pachyderma* $\delta^{18}O$ values and coiling ratios from the equivalent regional surface sediments. We then demonstrate the palaeoceanographic application of this relationship down-core.

The general modern hydrography of the Nordic seas is reflected in the stable oxygen isotope values of both *N. pachyderma* (sin.) and *N. pachyderma* (dex.)[21], since the $\delta^{18}O$ incorporated into test calcite is a function of temperature and salinity[22]. The $\delta^{18}O$ values of *N. pachyderma* (sin.) and *N. pachyderma* (dex.) are largely identical under polar conditions (Fig. 1b) in the western region, where relative abundances of *N. pachyderma* (dex.) are low (Fig. 1a). But in the east and south of the Nordic seas, where the percentage of *N. pachyderma* (dex.) increases rapidly under more-temperate conditions (Fig. 1a), a significant isotopic difference between left- and right-coiling *N. pachyderma* of up to about 1‰ in $\delta^{18}O$ is observed (Fig. 1b).

Molecular analysis of the small subunit (SSU) ribosomal RNA sequences has previously shown that the *N. pachyderma* morpho-

species consists of a complex of distinct genotypes[7], and that the coiling direction in the Southern Hemisphere is not a phenotypic response to temperature, but reflects genetic divergence and the probable existence of two separate species[7]. In this study (Fig. 2), we have found that throughout the Nordic seas, all left-coiling *N. pachyderma* are genotypically [Type I (sin.)]. This is not the case for *N. pachyderma* (dex.). In the region of the Norwegian Sea and Denmark Strait south of 64° N (Fig. 2), all *N. pachyderma* (dex.) are genotypically [Type I (dex.)] and are genetically highly distinct from the left-coiling variant[7]. Under polar conditions north of the latitude 70° N where the coiling ratios are confined to less than 5% (Fig. 1a) and the $\delta^{18}O$ values of *N. pachyderma* (sin.) and *N. pachyderma* (dex.) are largely the same (Fig. 1b), genotyping reveals that the left- and right-coiling variants of *N. pachyderma* are genotypically identical. Both are [Type I (sin.)]. Clearly, *N. pachyderma* [Type I (dex.)] is thriving in the relatively warm North Atlantic waters, and is adapted to a totally different hydrographic regime than left- and right-coiling [Type I (sin.)], which is dominant in polar waters. Such genetic and environmental evidence indicates that these two genetic types should be considered different species. As might be expected, there is a mixing zone between the right- and left-coiling provinces (70° N to 64° N) where the dextral morphotypes can be either *N. pachyderma* [Type I (dex.)] or [Type I (sin.)].

The genetic evidence for *N. pachyderma* shows that the morphological distinction of coiling directions is not sufficient to distinguish between genotypes. Since fossil specimens do not contain DNA for genetic analysis, we need an indicator proxy to distinguish between the two species of right-coiling *N. pachyderma*. From the presented sediment data in combination with the genetic evidence it can be assumed that in regions where the percentage of *N. pachyderma* (dex.) does not exceed a 'threshold' value of ~5% in coiling direction, both *N. pachyderma* coiling variants will be identical, genotypically [Type I (sin.)], with a correspondingly identical isotopic composition. In regions where the percentage of *N. pachyderma* (dex.) exceeds this 'threshold' value, *N. pachyderma*
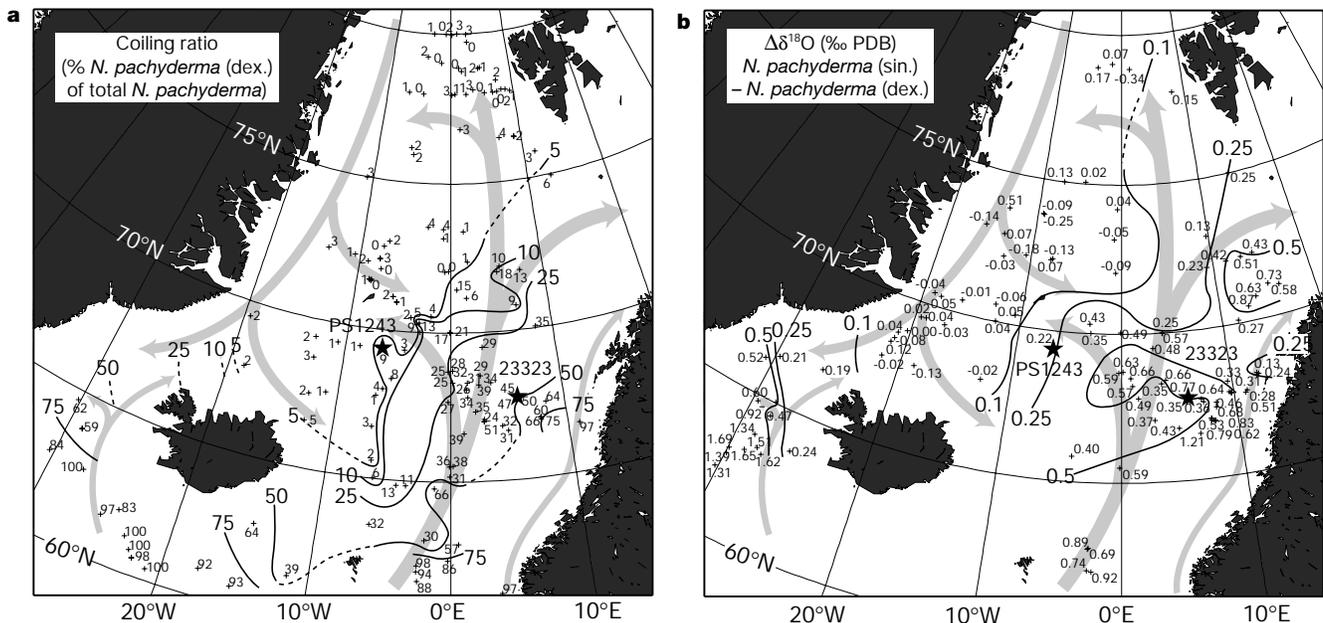


**Figure 1** Spatial distributions of coiling ratios and isotopic differences. **a**, Coiling ratios of *N. pachyderma* in surface sediments of the Nordic seas based on faunal census data (>150 μm)[10]. The core locations of PS1243 and M23323 are highlighted. The arrows show the general surface ocean currents: the southward-flowing cold East Greenland Current with side branches; the northward-flowing warm Norwegian Current with side

branches; also indicated are the warm Norwegian Coastal and Irminger currents along the Norwegian and Iceland coasts, respectively. **b**, Isotopic difference between *N. pachyderma* (sin.) and *N. pachyderma* (dex.) from surface sediments in the Nordic seas[21]. For each analysis, 20–30 shells have been measured from the size fraction 125–250 μm.
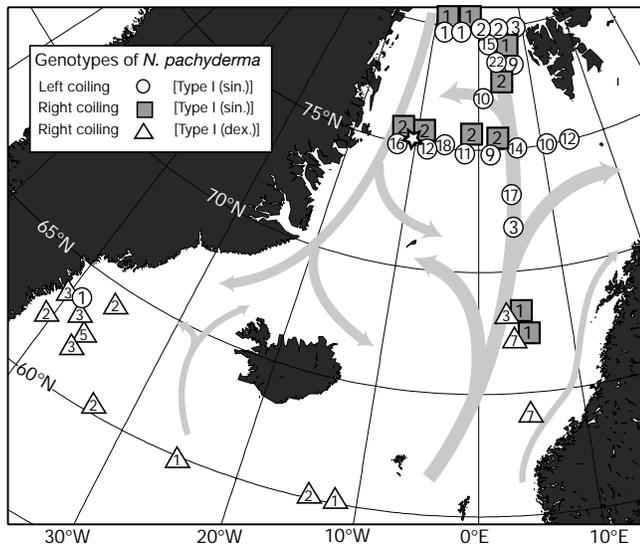
**Figure 2** Geographical distribution of genotypes of left-coiling *N. pachyderma* [Type I (sin.)], the right-coiling form of *N. pachyderma* [Type I (sin.)], and right-coiling *N. pachyderma* [Type I (dex.)]. Data from the Denmark Strait region are taken from ref. 8. Numbers within symbols indicate number of specimens genotyped at the specific locations. At a single position, marked with a star, there was sufficient suitable material in a multinet to derive an isotope signature for both left- and right-coiling *N. pachyderma* from the same plankton sample. Identical $\delta^{18}O$ and $\delta^{13}C$ values were found for both, corroborating our evidence that in this regional water mass they are the same genetic type.

(dex.) is expected to have a progressively different isotopic composition from *N. pachyderma* (sin.) as the *N. pachyderma* [Type I (dex.)] genotype increasingly dominates the assemblage.

In order to further test our conclusions from the modern data set, we investigated two sediment cores representing the warmer and colder regions of the Norwegian Sea (see Fig. 1 for locations). Samples from the glacial sections of the two cores show a low relative abundance (1–5%) of *N. pachyderma* (dex.) (Fig. 3). Since the early Holocene (~9–10 kyr ago), dextral coiling ratios are higher, with levels of 5–10% in core PS1243 and 40–60% in core M23323 due to climate warming at the end of the deglaciation. These faunal differences reflect the basic water-mass temperature gradient between the two sites. A similar picture is recognized in the stable oxygen isotope records of *N. pachyderma* (sin.) and *N. pachyderma* (dex.), which both depict the overall climatic change since the Last Glacial Maximum (LGM) (Fig. 3). However, while $\delta^{18}O$ in both species are nearly the same during the glacial sections, when dextral coiling ratios are extremely low, a systematic offset of about 0.5‰ is noted since about 10 kyr ago when dextral coiling ratios increase, accompanied by a decrease in the relative abundance of *N. pachyderma* (sin.) (Fig. 3). In light of the genotype evidence for the Nordic seas, this Holocene offset in $\delta^{18}O$ has to be interpreted as an alternation in the species of *N. pachyderma* (dex.) from [Type I (sin.)] during glacial times to a [Type I (dex.)] domination in the interglacial interval. The isotopic offset of about 0.5‰ diminishes in core PS1243 since about 4 kyr ago, and corresponds to a period of increasing abundance of *N. pachyderma* (sin.) and a coeval abundance decrease of *N. pachyderma* (dex.) fairly close to the threshold value of ~5% coiling ratio. This would result in a greater contribution of the right-coiling [Type I (sin.)] genotype to the $\delta^{18}O$ signal during this time in core PS1243, and explains the reduced offset in $\delta^{18}O$ between *N. pachyderma* (sin.) and *N. pachyderma* (dex.) compared to that of core M23323. Altogether this strongly supports our conclusion that a species-dependent isotopic shift in *N. pachyderma* (dex.) $\delta^{18}O$ signal can be inferred
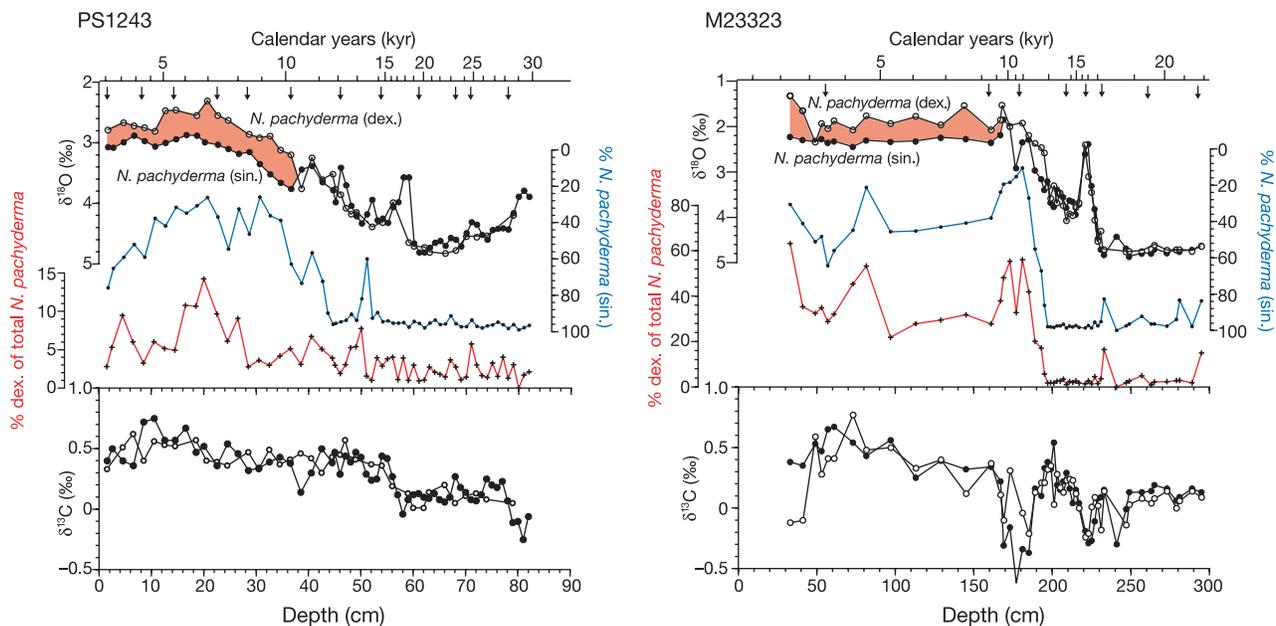


**Figure 3** Time series showing climate proxies of two sediment cores versus depth and versus calendar years. The age tie-points of calendar years[21,29] are indicated on top by arrows. Core P1243 is located close to the Arctic Front (69° N, 7° W). Core M23323 is located under the warm Norwegian Current on the Vøring Plateau (68° N, 6° E) (for core locations see Fig. 1). Top: $\delta^{18}O$ values of *N. pachyderma* (sin.) (filled circles) and *N. pachyderma* (dex.) (open circles; size fraction 125–250 μm). Middle: coiling ratio (*N. pachyderma* (dex.) as a percentage of total *N. pachyderma*) shown in red, and relative abundance of *N. pachyderma* (sin.) (given as a percentage of total planktonic species (size fraction >125 μm)) shown in blue; please note reversed *y*-axis for relative abundance of *N. pachyderma* (sin.). Bottom: $\delta^{13}C$ values of *N. pachyderma* (sin.) (filled circles) and *N. pachyderma* (dex.) (open circles; size fraction 125–250 μm).

when relative abundances of *N. pachyderma* (dex.) cross a specific threshold value of ~5%.

The δ^{18}O isotopic difference of 0.5‰ between the right-coiling forms of *N. pachyderma* [Type I (sin.)] and *N. pachyderma* [Type I (dex.)] in the Holocene translates into a temperature or salinity difference of approximately 2 °C or 2 practical salinity units, respectively. This isotopic difference is an additional increment, superimposed upon the global LGM/Holocene isotopic signature. For all future palaeoceanographic δ^{18}O isotope studies carried out on *N. pachyderma* (dex.) at low percentage coiling ratios in the Northern Hemisphere, it will be of considerable importance to account for this derived species dependent isotopic shift of up to ~0.5‰. Interestingly, while the δ^{18}O values reveal such a marked difference during the Holocene, there is no systematic offset in δ^{13}C between *N. pachyderma* (sin.) and *N. pachyderma* (dex.) over the entire time interval (Fig. 3). Since δ^{13}C values of foraminifers are thought to record specific environmental conditions[23,24], the Holocene δ^{18}O offset may represent a genotype-specific vital effect. However, we have shown that *N. pachyderma* [Type I (sin.)] and *N. pachyderma* [Type I (dex.)] are clearly adapted to different hydrographic regimes, and it remains to be determined whether the species-dependent δ^{18}O offset represents annual, seasonal or water-depth hydrological differences, a vital effect or a combination of them. Although our findings add yet another aspect to the interpretation of δ^{18}O values of planktonic foraminifers in the Northern Hemisphere, by using the indicator proxy of the coiling ratio, the correct interpretation can be deduced. Clearly the relevance of coiling ratios for isotope records of *N. pachyderma* (dex.) in other palaeoceanographically important regions needs to be addressed.

There is accumulating evidence that several morphospecies do not represent genetically continuous species over their entire environmental adaptive range, as newly discovered potential 'cryptic species' seem to have different environmental preferences[6–8,25]. Isotopic differences may also be associated with other genotypes of morphospecies commonly used in palaeoceanographic reconstructions[26,27]. An understanding of the nature of these adaptations will considerably enhance other palaeoceanographic and palaeoclimate proxies if the 'cryptic species' can be distinguished in the fossil record, as was possible for this study. □

## Methods

### Foraminiferal counts

In down-core sediment samples about 300 individuals of the size fraction >125 μm have been counted, while in surface sediment samples individuals >150 μm have been counted[10]. Comparison of counting results of these different size classes in the Nordic seas has shown that there is no significant difference in relative faunal abundances and thereby also coiling ratios[28]. In the *N. pachyderma* (sin.) dominated polar regions, typical coiling ratios of *N. pachyderma* (dex.) are between 1% and 5 ± 1% from counts of 300 individuals[10]. The upper value of 5% coiling ratio has been adopted as the threshold value for the start of the influx of *N. pachyderma* [Type I (dex.)] into the *N. pachyderma* [Type I (sin.)] fossil assemblage. This threshold conforms to the upper values observed in the polar-region core tops (Fig.1a), the glacial down-core sediments (Fig. 3), and is also approximately the threshold observed in core PS1243 at which the isotopic offset is observed to decrease in the later Holocene (Fig.3).

### Isotope analysis of calcite shells

About 20–30 individuals were picked from the 125–250 μm size fraction, and analysed at the Leibniz Laboratory of Kiel University using a fully automated Kiel Device plus MAT 251 isotope mass spectrometer system. Results are reported in the usual δ-notation relative to PDB, and have an accuracy of 0.07‰ and 0.04‰ for δ^{18}O and δ^{13}C, respectively.

### Sampling localities

Foraminifera were collected on board RV *Polarstern* (ARKXV/1 + 2); specimens were obtained using multinets (upper 500 m) at 75° N (from 13° W to 13° E), and from a mixture of multinet and surface pumped water samples in the Nordic seas between 80° N and 60° N.

### Isolation and sequencing of SSU gene fragments

DNA extraction, amplification by polymerase chain reaction (PCR) and automated sequencing of either a ~500-base-pair (bp) or a ~1,000-bp region of the terminal 3′ end of the foraminiferal SSU rRNA gene was as described previously[7,8]. The gene fragments for

*N. pachyderma* (dex.) were directly sequenced. Some limited degree of ambiguity was detected in the gene repeats for *N. pachyderma* (sin.), and consensus sequences were obtained by cloning using a pCR 2.1 TOPO TA cloning kit (Invitrogen) and then sequencing using universal primers.

1. Ericson, D. B. Coiling direction of *Globigerina pachyderma* as a climatic index. *Science* **130,** 219–220 (1959).
2. CLIMAP Project Members The surface of the ice-age Earth. *Science* **191,** 1131–1137 (1976).
3. Bond, G. C., Broecker, W., Johnsen, S. & McManus, J. Correlations between climate records from North Atlantic sediments and Greenland ice. *Nature* **365,** 143–147 (1993).
4. Bé, A. W. & Tolderlund, D. S. in *The Micropaleontology of the Oceans* (eds Funnel, B. M. & Riedel, W. R.) 105–149 (Cambridge Univ. Press, Cambridge, 1971).
5. Bandy, O. L. Origin and development of *Globorotalia (Turborotalia) pachyderma* (Ehrenberg). *Micropaleontology* **18,** 294–318 (1972).
6. de Vargas, C., Norris, R., Zaninetti, L., Gibb, S. W. & Pawlowski, J. Molecular evidence of cryptic speciation in planktonic foraminifers and their relation to oceanic provinces. *Proc. Natl Acad. Sci. USA* **96,** 2864–2868 (1999).
7. Darling, K. F. *et al.* Molecular evidence for genetic mixing of Arctic and Antarctic subpolar populations of planktonic foraminifers. *Nature* **404,** 43–47 (2000).
8. Stewart, I. A., Darling, K. F., Kroon, D., Wade, C. M. & Troelstra, S. R. Genotypic variability in subarctic Atlantic planktic foraminifera. *Mar. Micropaleontol.* **43,** 143–153 (2001).
9. Kipp, N. G. New transfer function for estimating past sea-surface conditions from sea-bed distribution of planktonic foraminiferal assemblages in the North Atlantic. *Geol. Soc. Mem.* **145,** 3–41 (1976).
10. Pflaumann, U., Duprat, J., Pujol, C. & Labeyrie, L. D. SIMMAX: A modern analog technique to deduce Atlantic sea surface temperatures from planktonic foraminifera in deep-sea sediments. *Paleoceanography* **11,** 15–35 (1996).
11. Healy-Williams, N., Williams, D. F. & Ehrlich, R. Quantifications of morphotypes in *Neogloboquadrina pachyderma* using Fourier shape analysis. *Antarct. J. US* **18,** 138–140 (1984).
12. Williams, D. F., Ehrlich, R., Spero, H. J., Healy-Williams, N. & Gary, A. C. Shape and isotopic differences between conspecific foraminiferal morphotypes and resolution of paleoceanographic results. *Palaeogeogr. Palaeoclimatol. Palaeoecol.* **64,** 153–162 (1988).
13. Cifelli, R. Observations of *Globigerina pachyderma* (Ehrenberg) and *Globigerina incompta* Cifelli from the North Atlantic Ocean. *J. Foram. Res.* **3,** 157–166 (1973).
14. Huber, R., Meggers, H., Baumann, K.-H., Raymo, M. E. & Henrich, R. Shell size variation of the planktonic foraminifer *Neogloboquadrina pachyderma* sin. in the Norwegian Greenland Sea during the last 1.3 Myrs: Implications for paleoceanographic reconstructions. *Palaeogeogr. Palaeoclimatol. Palaeoecol.* **160,** 193–212 (2000).
15. Kellogg, T., Duplessy, J. & Shackleton, N. Planktonic foraminiferal and oxygen isotopic stratigraphy and paleoclimatology of Norwegian Sea deep-sea cores. *Boreas* **7,** 61–73 (1978).
16. Jansen, E. The use of stable oxygen and carbon isotope stratigraphy as a dating tool. *Quat. Int.* **1,** 151–166 (1989).
17. Bauch, H. A. in *Land-ocean Systems in the Siberian Arctic: Dynamics and History* (eds Kassens, H. *et al.*) 601–613 (Springer, Berlin, 1999).
18. Oppo, D. W., McManus, J. F. & Cullen, J. L. Abrupt climate events 500,000 to 340,000 years ago: Evidence from subpolar North Atlantic sediments. *Science* **279,** 1335–1338 (1998).
19. McManus, J., Oppo, D. & Cullen, J. A 0.5-million-year record of millennial-scale climate variability in the North Atlantic. *Science* **283,** 971–975 (1999).
20. Oppo, D., Keigwin, L. D., McManus, J. F. & Cullen, J. L. Persistent suborbital climate variability in marine isotope stage 5 and Termination II. *Paleoceanography* **16,** 280–292 (2001).
21. Simstich, J. Die ozeanische Deckschicht des Europäischen Nordmeers im Abbild stabiler Isotope von Kalkgehäusen unterschiedlicher Planktonforaminiferenarten. *Ber.–Rep. Inst. Geowiss., Univ. Kiel* **2,** 1–96 (1999).
22. Emiliani, C. Pleistocene temperatures. *J. Geol.* **63,** 538–578 (1955).
23. Spero, H. J., Bijma, J., Bemis, B. & Lea, D. Effects of sea water carbonate chemistry on planktonic foraminifera carbon and oxygen isotope values. *Nature* **390,** 497–500 (1997).
24. Bauch, D., Erlenkeuser, H., Winckler, G., Pavlova, G. & Thiede, J. Carbon isotopes and habitat of polar planktic foraminifera in the Okhotsk Sea: The "Carbonate Ion Effect" under natural conditions. *Mar. Micropaleontol.* **45,** 83–99 (2002).
25. de Vargas, C., Renaud, S., Hilbrecht, H. & Pawlowski, J. Pleistocene adaptive radiation in *Globorotalia truncatulinoides*: Genetic, morphologic, and environmental evidence. *Paleobiology* **27,** 104–125 (2001).
26. Bemis, B. E., Spero, H. J. & Thunell, R. C. Using species-specific paleotemperature equations with foraminifera: A case study in the Southern California Bight. *Mar. Micropaleontol.* **46,** 405–430 (2002).
27. Darling, K. F., Kucera, M., Wade, C. M., von Langen, P. & Pak, D. Seasonal occurrence of genetic types of planktonic foraminiferal morphospecies in the Santa Barbara Channel. *Paleoceanography* **18,** 1032, doi: 10.1029/2001PA000723 (2003).
28. Kandiano, E. S. & Bauch, H. A. Implications of planktic foraminiferal size fractions for the glacial-interglacial paleoceanography of the polar North Atlantic. *J. Foram. Res.* **32,** 245–251 (2002).
29. Bauch, H. A. *et al.* A multiproxy reconstruction of the evolution of deep and surface waters in the subarctic Nordic seas over the last 30,000 years. *Quat. Sci. Rev.* **20,** 659–678 (2001).